JACS
JOURNAL OF THE AMERICAN CHEMICAL SOCIETY
Article
pubs.acs.org/JACS

Fluorophore Targeting to Cellular Proteins via Enzyme-Mediated Azide Ligation and Strain-Promoted Cycloaddition

Jennifer Z. Yao,[†] Chayasith Uttamapinant,[†] Andrei Poloukhtine,[‡] Jeremy M. Baskin,[§] Julian A. Codelli,[§] Ellen M. Sletten,[§] Carolyn R. Bertozzi,[§,∥,⊥] Vladimir V. Popik,[‡] and Alice Y. Ting*[,†]

[†]Department of Chemistry, Massachusetts Institute of Technology, 77 Massachusetts Avenue. Cambridge, Massachusetts 02139, United States

[‡]Department of Chemistry, University of Georgia, 212 Carlton Street. Athens, Georgia 30602, United States

[§]Departments of Chemistry and [∥]Molecular and Cell Biology and Howard Hughes Medical Institute, University of California, Berkeley, California 94720, United States

[⊥]The Molecular Foundry, Lawrence Berkeley National Laboratory, Berkeley, California 94720, United States

Supporting Information

ABSTRACT: Methods for targeting of small molecules to cellular proteins can allow imaging with fluorophores that are smaller, brighter, and more photostable than fluorescent proteins. Previously, we reported targeting of the blue fluorophore coumarin to cellular proteins fused to a 13-amino acid recognition sequence (LAP), catalyzed by a mutant of the *Escherichia coli* enzyme lipoic acid ligase (LplA). Here, we extend LplA-based labeling to green- and red-emitting fluorophores by employing a two-step targeting scheme. First, we found that the W37I mutant of LplA catalyzes site-specific ligation of 10-azidodecanoic acid to LAP in cells, in nearly quantitative yield after 30 min. Second, we evaluated a panel of five different cyclooctyne structures and found that fluorophore conjugates to aza-dibenzocyclooctyne (ADIBO) gave the highest and most specific derivatization of azide-conjugated LAP in cells. However, for targeting of hydrophobic fluorophores such as ATTO 647N, the hydrophobicity of ADIBO was detrimental, and superior targeting was achieved by conjugation to the less hydrophobic monofluorinated cyclooctyne (MOFO). Our optimized two-step enzymatic/chemical labeling scheme was used to tag and image a variety of LAP fusion proteins in multiple mammalian cell lines with diverse fluorophores including fluorescein, rhodamine, Alexa Fluor 568, ATTO 647N, and ATTO 655.

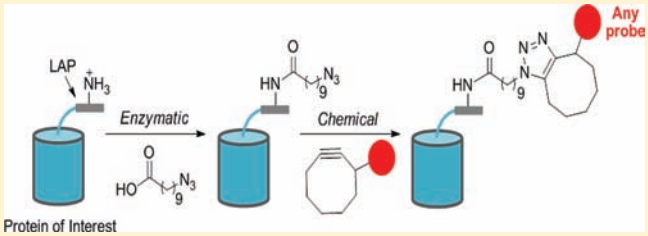

INTRODUCTION

The use of small-molecule fluorophores in live cells to replace fluorescent proteins has grown in recent years due to the need for improved photophysical properties for advanced imaging modalities such as single-molecule and super-resolution imaging,[1,2] and also because of the availability of new methods for targeting such probes to cellular proteins.[3] Our lab has been working to develop better protein labeling methods, because existing techniques still have significant shortcomings. HaloTag[4] and SNAP/CLIP[5] methods offer high labeling specificity but the tags are large, like fluorescent proteins, and can interfere with the trafficking and function of the proteins to which they are fused. FlAsH[6] uses a small peptide tag for labeling, but the specificity is imperfect, as we[7] and other labs[8] have shown. Several other methods, such as sortase,[9] Sfp/AcpS,[10] and aldehyde tag[11] are restricted to labeling of cell surface proteins rather than intracellular proteins.

Our lab has developed a protein labeling method based on enzyme-catalyzed probe ligation, called PRIME[7] (PRobe Incorporation Mediated by Enzymes). The platform for this method is the *Escherichia coli* enzyme lipoic acid ligase (LplA), which normally conjugates lipoic acid to a lysine side chain of one of its three natural acceptor proteins (Figure 1A).[12] We used *in vitro* evolution to engineer a 13-amino acid replacement for these acceptor proteins, called LAP[13] (LplA Acceptor Peptide), which can be genetically fused to any protein of interest. We then showed that mutagenesis of the lipoic acid binding pocket could allow LplA to ligate unnatural small molecules instead of lipoic acid, including 7-hydroxycoumarin,[7] 7-aminocoumarin,[14] Pacific Blue,[15] and aryl azide.[16] Coumarin ligation has been demonstrated in living cells and used to image various cytoskeletal proteins and neurexin.[7,14,15]

Though PRIME with coumarin ligase is versatile and specific, coumarin is a blue fluorophore with excitation and emission maxima of 387 and 448 nm,[7] which are not optimal for live cell imaging. Red-shifted fluorophores are more desirable as they enable higher signal to background ratios due to their greater separation from cellular autofluorescence. Furthermore, coumarin does not exhibit the useful photoswitching properties and higher photon count possessed by cyanine and ATTO

Received: September 1, 2011
Published: January 4, 2012

   dx.doi.org/10.1021/ja208090p | *J. Am. Chem. Soc.* 2012, 134, 3720–3728

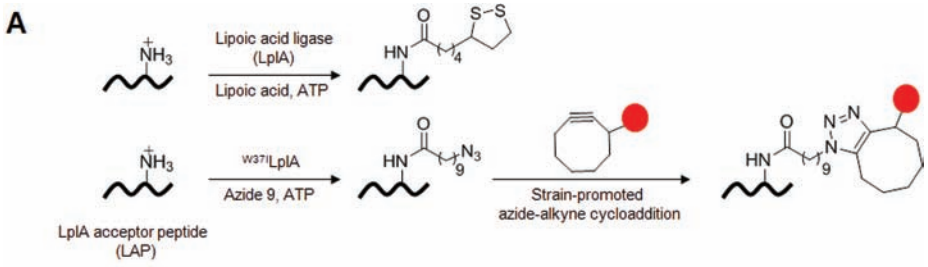

B

Probe		% Conversion to product with LplA variants						
		WT	W37G	W37A	W37V	W37I	W37L	W37S
	n=7 Azide 7	33%*	<3%	<3%	39%*	13%	<3%	N.D.
	n=8 Azide 8	6%	N.D.	N.D.	10%	5%	<3%	N.D.
	n=9 Azide 9	N.D.	5%	8%	89%*	53%*	<3%	N.D.
	n=10 Azide 10	N.D.	27%	11%	38%	9%	N.D.	N.D.

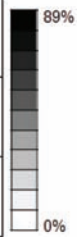

Figure 1. Fluorophore targeting via LplA-catalyzed azide ligation followed by strain-promoted azide-alkyne cycloaddition. (A) Top: natural ligation of lipoic acid catalyzed by wild-type LplA.[12] Bottom: two-step fluorophore targeting used in this work. First, the ^{W37I}LplA mutant ligates 10-azidodecanoic acid ("azide 9") onto the 13-amino acid LplA acceptor peptide (LAP).[13] Second, the azido moiety is chemoselectively derivatized using a cyclooctyne−fluorophore conjugate, via strain-promoted, copper-free [3 + 2] cycloaddition. The red circle represents any fluorophore or probe. (B) Screening to identify the best LplA mutant/azide substrate pair. The table shows percent conversions of LAP to the LAP−azide product conjugate. Wild-type LplA and six W37 point mutants were screened against four azidoalkanoic acid substrates of various lengths. N.D. indicates that product was not detected. Screening was performed with 100 nM ligase, 600 μM LAP, and 20 μM azide substrate for 20 min at 30 °C. Conversions were measured in duplicate. Note that ^{W37S}LplA was active with the natural substrate, lipoic acid (data not shown). The starred entries in the table were further evaluated in Figure 2.

dyes, which are necessary for super-resolution imaging by PALM and STORM techniques.[1,2,17]

The goal of this work is to generalize PRIME for labeling of intracellular proteins with diverse fluorophore structures. We wanted a general strategy for targeting to intracellular LAP-fused proteins any fluorophore that can cross the cellular membrane and exhibit minimal nonspecific binding or reactivity to endogenous proteins.

To accomplish this, we needed an alternative approach to lipoic acid binding pocket mutagenesis. Most green and red fluorophores such as fluorescein, rhodamine, cyanine, and ATTO dyes are much larger than coumarin, the largest unnatural substrate so far to be recognized by an LplA mutant.[7] The crystal structure of LplA in complex with lipoyl-AMP ester, the intermediate of the natural ligation reaction, shows that the lipoyl moiety is completely enclosed within a binding pocket in the center of the enzyme.[18] Engineering an "exit tunnel" from this binding pocket to accommodate structures much larger than lipoic acid or coumarin is not straightforward.

Our approach was instead to use a two-step targeting scheme in which we first use LplA to ligate a "functional group handle" to a LAP fusion protein and then chemoselectively derivatize the functional group on LAP with a suitably derivatized fluorophore. We have previously accomplished such two-step labeling with LplA for cell surface proteins,[19] using an alkyl azide substrate for wild-type LplA and derivatizing the resulting LAP−azide conjugate with a monofluorinated cyclooctyne[20] (MOFO)−fluorophore conjugate. Here, we addressed several challenges to successfully implement a similar two-step labeling scheme inside living cells (Figure 1A, bottom). First, the LplA enzyme was expressed inside the cell instead of exogenously added to the cell media. Second, the azide ligation step was optimized to give maximum yield, while leaving minimal residual azide probe, which would interfere with the subsequent derivatization if it could not be completely removed from cells. This optimization required the use of a different LplA mutant/azide probe pair with improved kinetic properties. Third, we developed a protocol to remove excess unconjugated alkyl azide as completely as possible. Finally, we investigated a variety of cyclooctyne structures to select the ones with the best reactivity and specificity for LAP−azide.

Our experiments ultimately yielded a two-step targeting protocol using ^{W37I}LplA to ligate a 10-azidodecanoic acid ("azide 9") substrate to LAP inside living cells with nearly quantitative yield in 30 min. Excess unligated azide is removed with two rounds of media changes over 1 h. Out of five cyclooctyne structures tested, the aza-dibenzocyclooctyne, ADIBO[21,22] was generally the best, giving the highest signal for a variety of LAP fusion proteins in multiple cell types. However, because ADIBO is fairly hydrophobic, we found that it gives background when conjugated to more hydrophobic fluorophores such as ATTO 647N, in which case an alternative, less hydrophobic cyclooctyne, MOFO,[20] is preferred. Our two-step targeting protocol was successfully used to label multiple LAP fusion proteins in living mammalian cells with small-molecule fluorophores, ranging from fluorescein to ATTO 647N.

dx.doi.org/10.1021/ja208090p | J. Am. Chem. Soc. 2012, 134, 3720−3728

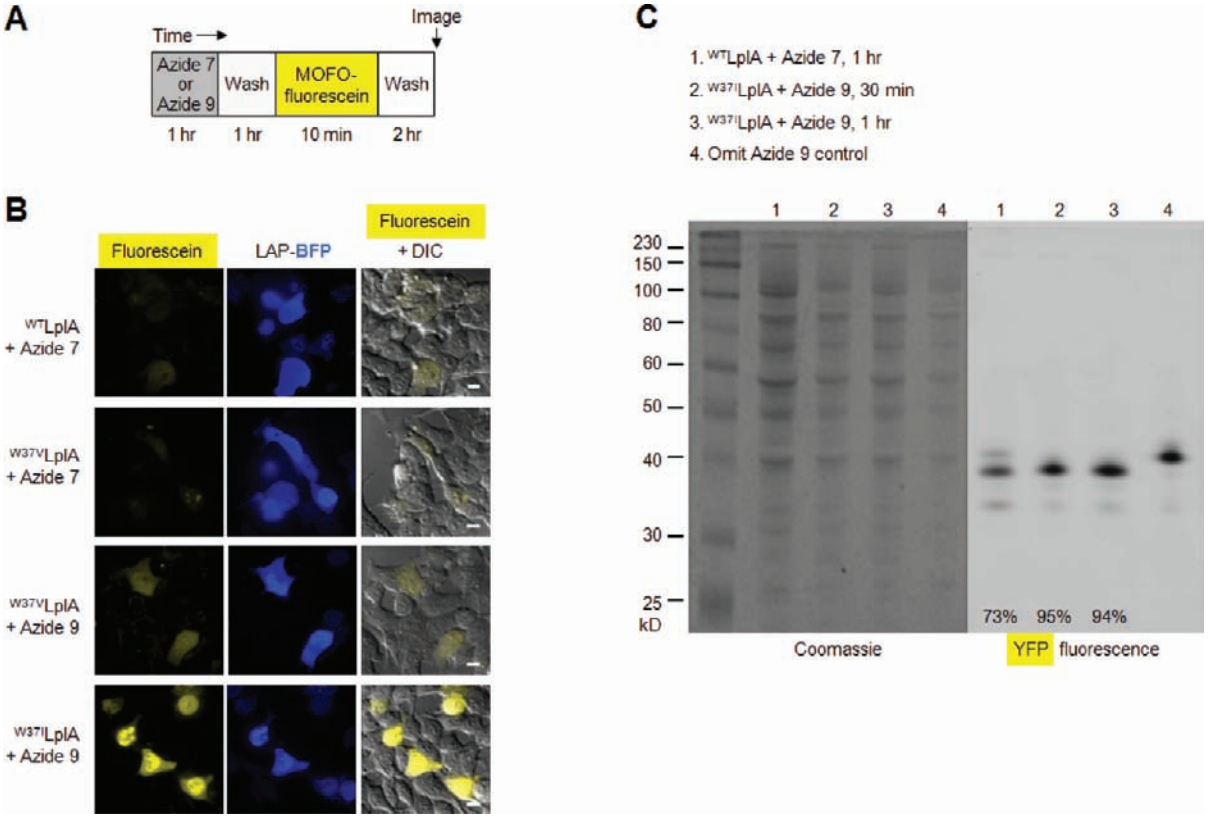

Figure 2. Identification of the best LplA mutant/azide substrate pair for intracellular protein labeling. (A) Labeling protocol. HEK cells coexpressing LplA and LAP-tagged BFP were labeled with azide 7 or azide 9 for 1 h, washed for 1 h, then labeled with monofluorinated cyclooctyne (MOFO) conjugated to fluorescein diacetate for 10 min. Thereafter, cells were washed again for 2 h to remove excess unconjugated fluorophore. (B) Images of HEK cells labeled as in (A), with different LplA mutant/azide probe pairs (starred combinations in Figure 1B). Scale bars, 10 μm. Quantitation of this data is shown in Figure S2A. A repeat of this experiment, with immunofluorescence staining to compare LplA expression levels, is shown in Figure S2B. Note that 10 times more ^{W37I}LplA plasmid was required to give similar expression levels to ^{WT}LplA and ^{W37I}LplA. (C) Gel-shift analysis of azide ligation in cells. HEK cells were prepared and labeled as in (A), except LAP−BFP was replaced by LAP−YFP. After azide ligation and the first wash, cells were lysed and run on a native 12% polyacrylamide gel. Labeled LAP-YFP runs faster than unlabeled LAP−YFP due to removal of a positive charge. Percent conversions to azide-LAP-YFP product are given at the bottom of the YFP fluorescence gel image. Lane 4 shows a negative control with azide 9 omitted. Additional controls are shown in Figure S4A.

METHODS

***In vitro* Azide Ligation.** For the screen in Figure 1B, reactions containing 100 nM LplA enzyme, 20 μM alkyl azide probe, 600 μM LAP peptide (sequence: H_2N-GFEIDKVWYDLDA-CO_2H), 2 mM ATP, and 2 mM magnesium acetate in 25 mM Na_2HPO_4 pH 7.2 were incubated at 30 °C for 20 min. Reactions were quenched with 40 mM EDTA (ethylenediaminetetraacetic acid, final concentration). Percent conversion to LAP−azide adduct was determined by HPLC with a C18 reverse phase column, recording absorbance at 210 nm. Elution conditions were 30−60% acetonitrile in water with 0.1% trifluoroacetic acid over 20 min at 1.0 mL/min flow rate. The percent conversion was calculated from the ratio of LAP−azide to sum of (unmodified LAP + LAP−azide). For Figure S3A in the Supporting Information (SI), reactions containing 1 μM LplA enzyme, 500 μM azide 9, and 300 μM LAP peptide were incubated at 30 °C for 2 h. For the kinetic measurements in Figure S3C, reactions containing 100 nM ^{W37I}LplA, 25−700 μM azide 9, and 600 μM LAP peptide were incubated at 30 °C, before quenching at various time points with EDTA.

Mammalian Cell Culture and Transfection. HEK, HeLa, and COS-7 cells were cultured in Modified Eagle medium (MEM; Cellgro) supplemented with 10% v/v fetal bovine serum (FBS; PAA Laboratories). All cells were maintained at 37 °C under 5% CO_2. For imaging, cells were plated on 5 mm × 5 mm glass coverslips placed within wells of a 48-well cell culture plate (0.95 cm^2 per well) 12−16 h prior to transfection. HEK cells were plated on glass precoated with 50 μg/mL fibronectin (Millipore) to increase adherence. In general, cells were transfected with 200 ng ^{W37I}LplA plasmid and 400 ng LAP fusion plasmid using Lipofectamine 2000 (Invitrogen) at 50−70% confluency. For Figures 2B and S2B, ^{WT}LplA and ^{W37V}LplA plasmids were introduced at 20 ng rather than 200 ng, to give comparable expression levels to ^{W37I}LplA (at 200 ng), since the former express much more strongly (Figure S2C).

General Protocol for Intracellular Protein Labeling. Sixteen to twenty hours after transfection, mammalian cells were incubated in complete media (10% FBS in MEM) containing 200 μM azide 9 for 1−2 h at 37 °C. To wash out excess azide 9, cells were rinsed three times with fresh, prewarmed complete media every 30 min for 1−1.5 h in total. Cells were then incubated with FBS-free MEM containing 10 μM cyclooctyne−fluorophore conjugate for 10 min at 37 °C, followed by rinsing three times with MEM over 5 min. Thereafter, cells were switched to fresh, prewarmed complete media, and the media was changed every 30 min to 1 h, for 1.5 to 8 h at 37 °C, prior to imaging. We have not observed any morphological changes in the cells during the washout period. ATTO 647N and ATTO 655 conjugates were loaded at 1 μM instead of 10 μM.

Cell Imaging. Cells were imaged in Dulbecco's phosphate buffered saline (DPBS) on glass coverslips at room temperature. For confocal imaging, we used a ZeissAxioObserver inverted microscope with a 60× oil-immersion objective, outfitted with a Yokogawa spinning disk confocal head, a Quadband notch dichroic mirror (405/488/568/647), and 405 (diode), 491 (DPSS), 561 (DPSS), and 640 nm (diode) lasers (all 50 mW). BFP (excitation 405 nm; emission 445/40 nm), YFP/fluorescein/Oregon Green 488 (excitation 491 nm; emission

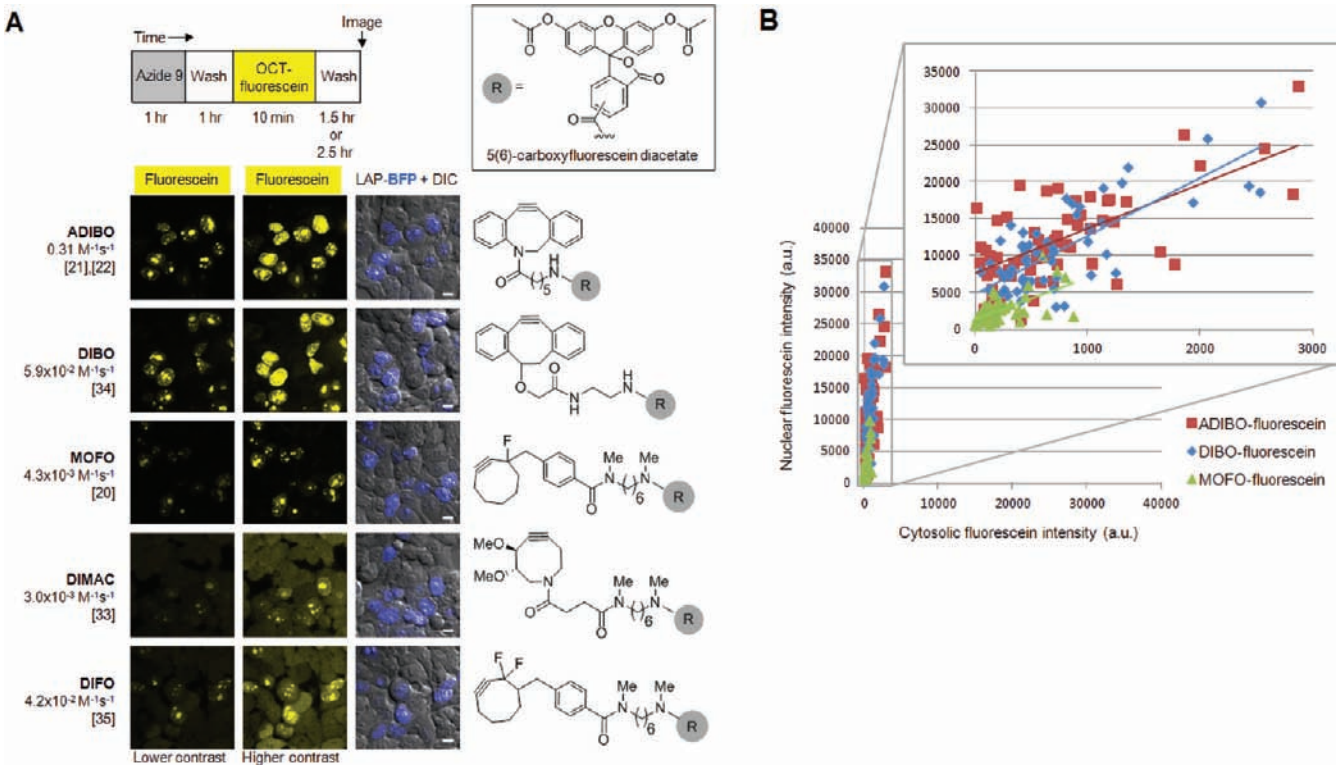

Figure 3. Evaluation of various cyclooctyne structures for site-specific intracellular protein labeling. (A) Top: labeling protocol for HEK cells coexpressing ^{W37I}LplA and nuclear-localized LAP−BFP (LAP−BFP−NLS). After labeling with azide 9 for 1 h and washing for 1 h, cells were treated with the indicated cyclooctyne-fluorescein conjugate for 10 min. Cells were washed again for 2.5 h to remove excess unconjugated fluorophore, except for MOFO, which was washed for only 1.5 h. Bottom: images of labeled HEK cells. The LAP−BFP−NLS image is overlaid on the DIC image. Fluorescein signal intensities can be compared in the first two columns, which show the fluorescein images at lower contrast (left) and higher contrast (middle). Cyclooctyne structures are shown at right, and second-order rate constants (with references below) are shown at left. ADIBO, aza-dibenzocyclooctyne; DIBO, 4-dibenzocyclooctynol; MOFO, monofluorinated cyclooctyne; DIMAC, 6,7-dimethoxyazacyclooct-4-yne; DIFO, difluorinated cyclooctyne. All scale bars, 10 μm. (B) Quantitation of data in (A). For the top three cyclooctynes (ADIBO, DIBO, and MOFO), the mean nuclear fluorescein intensity (representing specific labeling) was plotted against the mean cytosolic fluorescein intensity (representing nonspecific labeling), for the same cell. More than 50 single cells were analyzed for each cyclooctyne.

528/38 nm), Alexa Fluor 568/TMR/X-rhodamine (excitation 561 nm; emission 617/73 nm), and Alexa Fluor 647/ATTO 647N/ATTO 655 (excitation 640 nm; emission 700/75 nm) images were acquired using Slidebook 5.0 software (Intelligent Imaging Innovations). Acquisition times ranged from 100 ms to 3 s. Fluorophore intensities in each experiment were normalized to the same intensity ranges.

RESULTS

Screening for the Best Alkyl Azide Ligase. To generalize PRIME for targeting of diverse fluorophore structures, our first challenge was to develop a method to efficiently and specifically ligate a functional group handle to LAP fusion proteins inside living cells. Previously we reported that wild-type LplA can catalyze the conjugation of 8-azidooctanoic acid ("azide 7") to LAP with a k_{cat} of 6.66 min^{-1} and K_m of 127 μM.[19] This works well for cell surface labeling, where the azide probe can be added at high concentrations and then excess unligated probe can be easily washed away. For intracellular labeling, however, it is more difficult to thoroughly wash away excess unused probe. It is therefore preferable to deliver the azide probe at lower concentrations so that less residual azide remains after the ligation reaction, to minimize interference with the subsequent [3+2] cycloaddition. To use lower azide concentrations, without sacrificing azide ligation yield, we needed to engineer the LplA-catalyzed azide ligation reaction to improve its kinetic properties.

Previous work has shown that Trp37 in the lipoic acid binding pocket serves as a "gatekeeper" residue, and its mutation to smaller side chains allows LplA to recognize a variety of unnatural substrates.[7,14−16] To identify an improved LplA/azide pair, we prepared a panel of LplA Trp37 mutants (W37G, A, V, I, L, and S) and screened them against a panel of alkyl azide substrates of various lengths (Figure 1B). An HPLC assay was used to determine the percent conversion of LAP into LAP−azide conjugate, using 20 μM probe for 20 min (Figure 1B). We found that wild-type LplA and ^{W37V}LplA were the best ligases for the shortest azide 7 probe. For the longer probes, wild-type LplA was no longer effective, and ^{W37V}LplA and ^{W37I}LplA mutants were best. The four best ligase/probe pairs are starred in Figure 1B.

To differentiate between these top four ligase/azide pairs, we tested their performance in living cells. Human embryonic kidney (HEK) cells were transfected with plasmids for each LplA mutant and LAP−BFP (blue fluorescent protein). Azide 9 was added to the cells for 1 h. We empirically optimized the washout time required to fully remove excess azide, using cyclooctyne−fluorescein retention as a readout, and found that 1 h was adequate (Figure S1A). Therefore excess azide 7 and azide 9 were each washed from cells for 1 h, before addition of monofluorinated cyclooctyne (MOFO), conjugated to fluo-

dx.doi.org/10.1021/ja208090p | J. Am. Chem. Soc. 2012, 134, 3720−3728

rescein diacetate (structure in Figure 3A), to derivatize the azide−LAPs.

Following the labeling protocol shown in Figure 2A, after 10 min incubation and 2 h of washing to remove excess fluorophore, cells were imaged. Figure 2B shows specific labeling of LAP−BFP for all four combinations, but the highest signal-to-background ratio was obtained for the ^{W37I}LplA/azide 9 pair. Note the substantial improvement in signal intensity (~4-fold greater on average) compared to the wild-type LplA/azide 7 pair previously used for cell surface protein labeling.[19] These differences are quantified in Figure S2A, in which fluorescein intensity is plotted against LAP−BFP expression level for >100 single cells for each condition. Anti-FLAG immunofluorescence staining to detect FLAG-tagged LplA in cells showed that ligase expression levels are all comparable under our experimental conditions (Figure S2B).

We also used a gel shift assay as a separate readout of azide ligation yield inside cells (Figures 2C and S4A). HEK cells were prepared expressing LAP−YFP (yellow fluorescent protein) and either wild-type LplA or ^{W37I}LplA. Azide 7 or azide 9 was added for 30 min or 1 h before washing and cell lysis. The yield of azide ligation to LAP−YFP was determined by shift on a native polyacrylamide gel. The unmodified fusion protein, visualized by YFP fluorescence, runs at an apparent molecular weight of ~42 kD. Upon modification, the positively charged lysine of LAP converts into a neutral amide, and the apparent molecular weight of the fusion protein shifts down to ~38 kD. Using densitometry, we found that the ^{WT}LplA/azide 7 pair gave 73% ligation yield after 1 h labeling in cells, whereas the ^{W37I}LplA/azide 9 pair gave nearly quantitative ligation after only 30 min of azide 9 incubation. On the basis of these data and the cell imaging results, we selected ^{W37I}LplA/azide 9 as our best ligase/azide pair.

Characterization of the Azide 9 Ligase, ^{W37I}LplA. We proceeded to fully characterize our best azide ligation reaction. Figure S3A shows an HPLC analysis of ^{W37I}LplA-catalyzed ligation of azide 9 onto purified LAP peptide. The identity of the LAP−azide 9 product peak was confirmed by mass spectrometry (Figure S3B). Negative control reactions with ATP omitted or wild-type LplA in place of ^{W37I}LplA were also ran and showed no product formation. We also used HPLC to quantify product amounts in order to measure k_{cat} and K_m values. Figure S3C shows the Michaelis−Menten plot giving a k_{cat} of 3.62 min^{-1} and a K_m of 35 μM for azide 9 ligation to LAP catalyzed by ^{W37I}LplA. Compared to our previously reported azide 7 ligation, catalyzed by wild-type LplA,[19] this K_m is 4-fold lower. The k_{cat} is 1.8-fold reduced, giving an overall 2-fold improvement in k_{cat}/K_m.

Comparison of Cyclooctyne Structures. Next, we focused on the optimization of the azide derivatization chemistry in cells. Numerous bioorthogonal ligation reactions have been reported to derivatize alkyl azides, including the Staudinger ligation,[23] and copper-catalyzed[24] as well as strain-promoted[25] [3+2] azide−alkyne cycloadditions. Of these, copper-catalyzed [3+2] cycloaddition is the fastest, but copper(I) is toxic to cells[26] and not easily delivered into the cytosol, where it also could become sequestered by endogenous thiols. On the other hand, copper-free, strain-promoted cycloaddition has been successfully demonstrated inside living cells,[27−29] and on the surface of cells within living animals.[30−32] For this reason, we selected cyclooctyne−fluorophore conjugates to derivatize LAP−azide.

Numerous cyclooctyne structures have been developed by our laboratories[20,22,33−36] and other laboratories.[21,37] These structures vary in terms of ring strain and electron deficiency, which in turn affect reactivity and specificity. In addition, more hydrophilic cyclooctyne structures have been developed[33] to reduce the extent of nonspecific hydrophobic binding to cells. Because it was not clear which cyclooctyne structure(s) would be the best for our purpose, we selected a panel of five structures, derivatized each with 5(6)-carboxyfluorescein diacetate (Figure 3A), and compared the performance of these conjugates for LAP−azide labeling inside living cells.

Figure 3A shows that, for labeling of LAP−BFP−NLS (NLS is a nuclear localization signal) in HEK cells, ADIBO− and DIBO−fluorescein diacetate conjugates give the highest signal, consistent with their superior second-order rate constants (0.31 M^{-1} s^{-1} and 5.9 × 10^{-2} M^{-1} s^{-1}, respectively[21,34]). Surprisingly, significant nonspecific labeling is seen with DIMAC, even in untransfected cells, despite its more hydrophilic structure.[33] Most of this nonspecific signal can be washed away after cells are fixed, suggesting that it arises from nonspecific binding rather than covalent labeling (Figure S5A). DIFO[35] also gave background, which unlike DIMAC, persisted to some extent after cell fixation (Figure S5A); this may reflect covalent addition to endogenous cellular nucleophiles such as glutathione, which has previously been observed.[27,32] Lowering the DIFO−fluorescein diacetate concentration by 10-fold to 1 μM, and shortening the labeling time to 40 s reduced the background somewhat, but it was still higher than the background seen with ADIBO and DIBO (data not shown).

Labeling with MOFO-fluorescein diacetate was specific, like with ADIBO and DIBO, although the signal was lower, consistent with MOFO's slower rate constant (4.3 × 10^{-3} M^{-1} s^{-1}).[20] We quantitatively analyzed the signal-to-background ratios resulting from cellular labeling with ADIBO, DIBO, and MOFO, by calculating the cytosolic to nuclear signal intensity ratios for >50 single cells from each condition. Because the LAP fusion is nuclear-localized, a nuclear fluorescein signal represents specific labeling, whereas cytosolic fluorescein signal represents nonspecific background. Figure 3B shows that while absolute signals are ~4-fold higher with ADIBO and DIBO compared to MOFO, the signal-to-background ratios are comparable for all three cyclooctynes. We hypothesize that MOFO gives lower background because it is not as hydrophobic as ADIBO and DIBO. This is supported by the fact that shorter dye washout time is required for MOFO (1.5 h) compared to ADIBO and DIBO (2.5 h).

On the basis of these results, we selected ADIBO and DIBO for most of our cellular protein labeling experiments. However, as shown later, due to ADIBO's hydrophobicity, we find that MOFO is a better option when working with very hydrophobic fluorophores such as ATTO 647N.

Intracellular Protein Labeling with Azide 9 Ligase and ADIBO-Fluorescein. Having optimized both the azide ligase and the cyclooctyne, we proceeded to characterize two-step labeling inside cells and explore its generality. HEK cells expressing ^{W37I}LplA and LAP−BFP were labeled with azide 9 for 1 h followed by ADIBO−fluorescein diacetate. We empirically optimized the ADIBO−fluorophore loading concentration and washout time (Figure S1B). Since cycloaddition yield in cells increases with cyclooctyne concentration, we determined the highest concentration that we could load and yet obtain a clean washout in a reasonable period of time. We

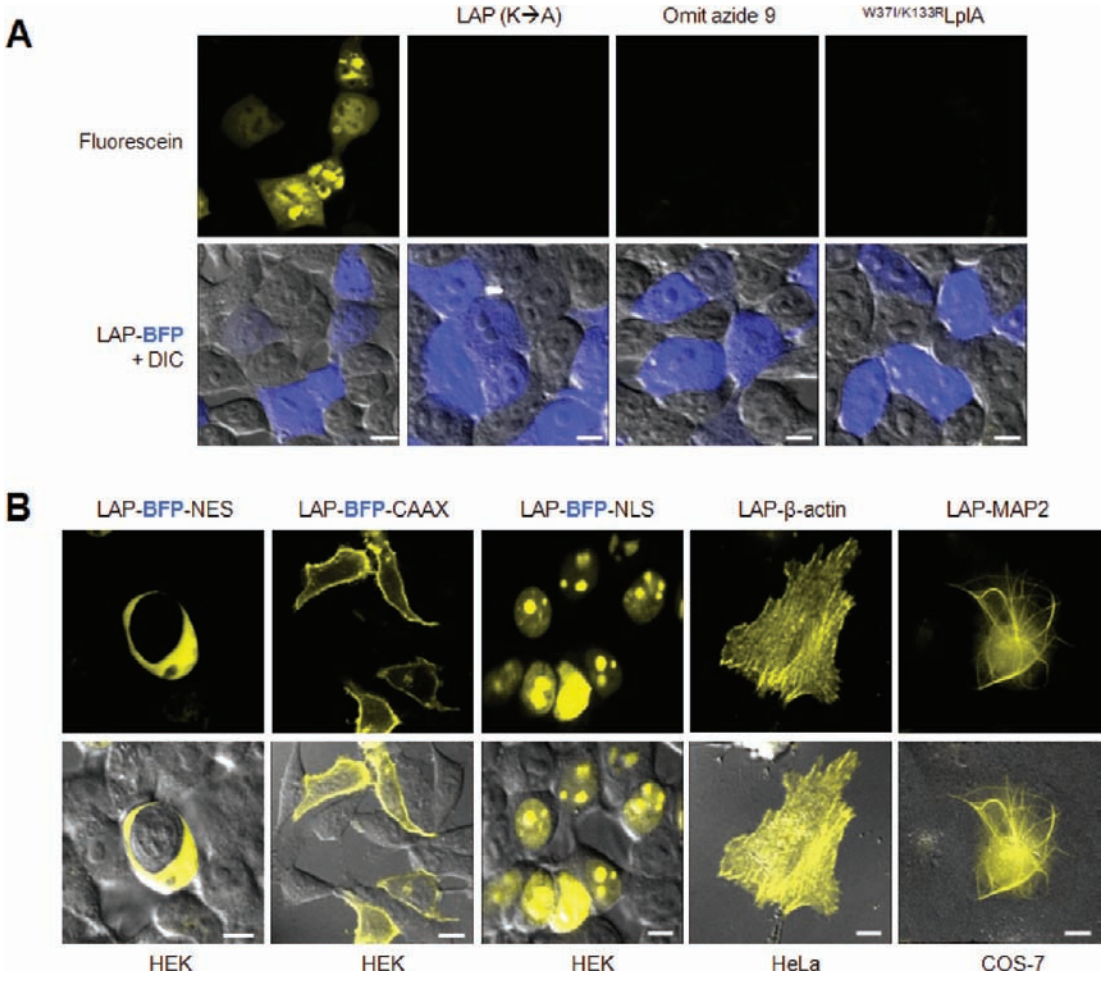

Figure 4. Intracellular protein labeling with azide 9 ligase and ADIBO−fluorescein. (A) HEK cells coexpressing ^{W37I}LplA and LAP−BFP were labeled with azide 9 and ADIBO−fluorescein as in Figure 3A, then imaged live. Negative controls are shown with an alanine mutation in LAP, azide 9 omitted, and a catalytically inactive mutant of LplA (last column). (B) ADIBO−fluorescein labeling of three localized LAP−BFP fusions, LAP−β-actin, and LAP−MAP2 (microtubule-associated protein 2). Labeling in the cell type indicated beneath each image was performed as in Figure 3A, except that for LAP−β-actin and LAP−MAP2, azide 9 was incubated for 2 h, and washed for 1.5 h before fluorophore addition. NES = nuclear export sequence; CAAX = prenylation tag; NLS = nuclear localization sequence. All scale bars, 10 μm.

found that 10 μM of ADIBO−fluorescein diacetate, followed by 2.5 h of washout, was optimal.

Figure 4A shows that HEK cells expressing LAP−BFP were labeled with ADIBO-fluorescein, whereas neighboring untransfected cells were not labeled. Negative controls with azide 9 omitted, LAP mutated, or a catalytically inactive LplA mutant, $^{W37I/K133R}$LplA,[18] did not show fluorescein labeling.

We also tested labeling of different LAP fusion proteins (Figure 4B). Using the two-step protocol shown in Figure 3A, we successfully labeled LAP in the nucleus, cytosol, and plasma membrane, as well as LAP fusions to β-actin and MAP2 (microtubule-associated protein 2). These experiments were performed in multiple mammalian cell lines (HEK, HeLa, and COS-7), demonstrating the versatility of the method.

Extension to Diverse Fluorophore Structures. To test our method with other fluorophores, we prepared ADIBO conjugates to tetramethylrhodamine (TMR), ATTO 647N, and ATTO 655. ADIBO−TMR and ADIBO−ATTO 655 both gave specific labeling (Figure 5A), but ADIBO−ATTO 647N produced a high level of nonspecific background. We hypothesized that this is due to the hydrophobicity of ATTO 647N (structure in Supporting Information). Even by itself, without a conjugated cyclooctyne, we have found that ATTO 647N gives a high level of nonspecific cell staining, primarily in the mitochondria, which is known to concentrate positively charged hydrophobic dyes (data not shown). We wondered if replacing ADIBO with the less hydrophobic cyclooctyne MOFO might reduce the background. Figure 5B shows a comparison of LAP−BFP−NLS labeling with ADIBO- and MOFO-conjugates to ATTO 647N. The graph on the right plots the specific labeling (nuclear ATTO signal) against the nonspecific labeling (cytosolic ATTO signal) for >50 single cells for each probe. It can be seen that MOFO−ATTO 647N gives more specific labeling than ADIBO−ATTO 647N, likely because the total hydrophobicity of the conjugate is reduced. This permitted us to perform MOFO−ATTO 647N labeling of LAP−β-actin in live COS-7 cells (Figure 5A).

We also tested the effect of varying the linker structure between MOFO and ATTO 647N in an attempt to further reduce the labeling background. The *N*,*N*′-dimethyl-1,6-hexanediamine (HDDA) linker that we used for most fluorophore conjugates in this work was replaced by a more hydrophilic polyethylene glycol (PEG) linker. Figure S5B shows that for labeling of LAP−BFP−NLS, no significant reduction in staining background was observed with MOFO−PEG−ATTO 647N, suggesting that the cyclooctyne and

dx.doi.org/10.1021/ja208090p | *J. Am. Chem. Soc.* 2012, 134, 3720−3728

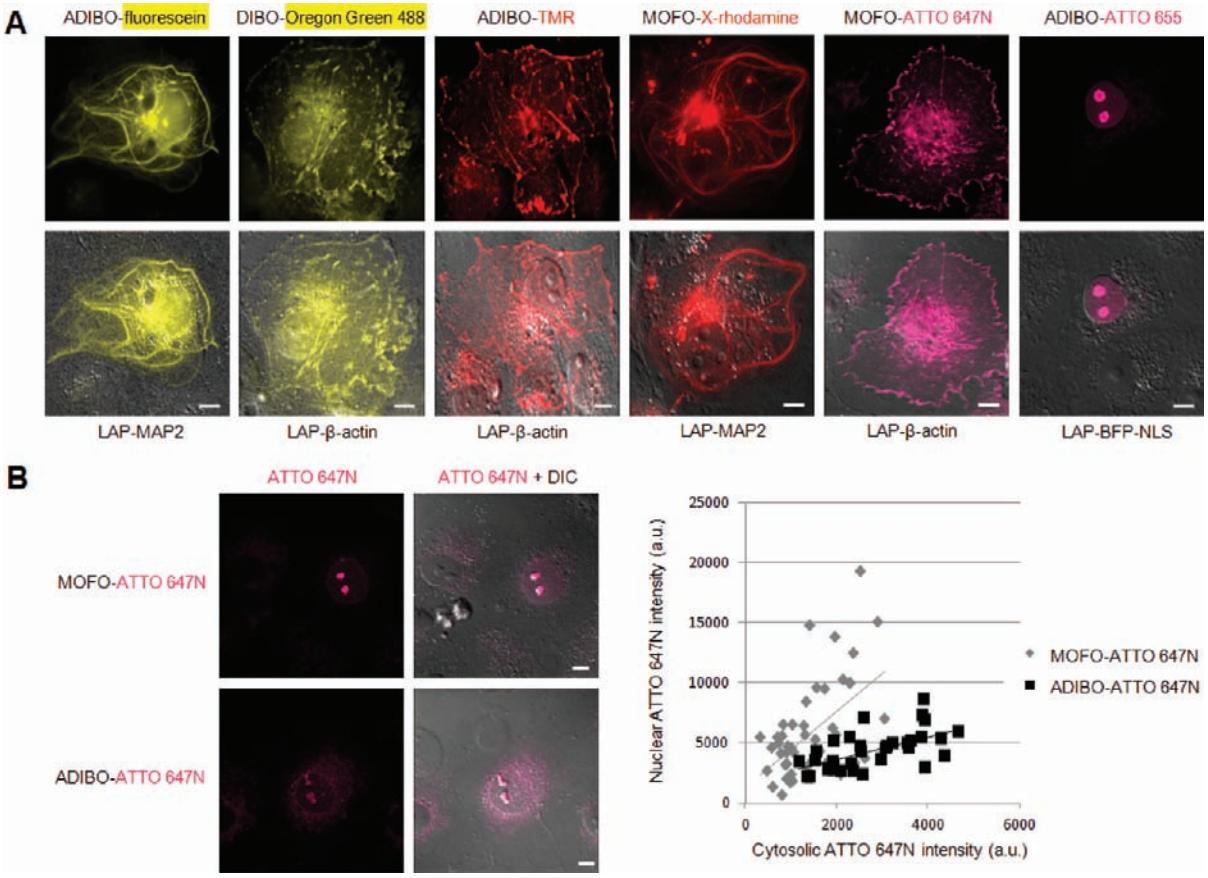

Figure 5. Intracellular protein labeling with diverse fluorophore structures. (A) COS-7 cells coexpressing ^{W37I}LplA and the indicated LAP fusion protein (labeled across bottom) were labeled with azide 9, followed by the indicated cyclooctyne–fluorophore conjugate (labeled across top). MOFO was used for the more hydrophobic fluorophores (X-rhodamine and ATTO 647N); ADIBO and DIBO were used for the others. Chemical structures are shown in the Supporting Information. TMR = tetramethylrhodamine. (B) Comparison of labeling specificity with ATTO 647N conjugates to MOFO and ADIBO. After labeling of COS-7 cells expressing nuclear-localized LAP–BFP–NLS with azide 9 and the indicated cyclooctyne–ATTO 647N conjugate, the mean nuclear ATTO 647N intensity (representing specific signal) was plotted against the mean cytosolic ATTO 647N intensity (representing nonspecific signal), for the same cell, for >50 single cells for each condition. Images are shown after 8 h of ATTO 647N conjugates washout. All scale bars, 10 μm.

fluorophore moieties dominate the hydrophobic properties of the probe.

Figure 5A shows live cell labeling of multiple LAP fusion proteins with a diverse palette of fluorophores. ADIBO is used for the more hydrophilic dyes such as fluorescein, TMR, and ATTO 655. DIBO is used for Oregon Green 488. MOFO is used for the more hydrophobic dyes, X-rhodamine and ATTO 647N.

Cell Surface Labeling and Measurement of Two-Step Ligation Yield in Cells. In addition to intracellular labeling, we performed cell surface labeling using commercially available cyclooctyne-probe conjugates (Figure S6A). LAP-tagged LDL receptor and neurexin-1β were labeled on the surface of HEK cells, by adding purified ^{W37I}LplA, azide 9, and ATP to the cell medium for 20 min. Thereafter, LAP–azide was derivatized using either membrane-impermeant DIBO–Alexa Fluor 647, or DIBO–biotin. The DIBO–biotin was visualized by staining with streptavidin–Alexa Fluor conjugates. Specific, azide-dependent cell surface labeling was seen in all cases.

Because DIBO–biotin is membrane-permeant, it is also possible to perform this labeling inside cells, although biotinylated LAP proteins can only be detected after membrane permeabilization and streptavidin staining. Figure S6B shows intracellular labeling in HEK cells coexpressing LAP–BFP–NLS and ^{W37I}LplA. After azide ligation, DIBO–biotin was added for 10 min; then cells were washed and fixed, and biotinylated LAP was detected with streptavidin-Alexa Fluor 568.

We used this two-step intracellular azide 9/DIBO–biotin labeling to measure our overall two-step labeling yield in cells. After performing labeling using the protocol in Figure 3A, HEK cells were lysed, incubated with excess streptavidin protein to bind biotinylated LAP–mCherry fusion protein, and the lysate was analyzed by gel. In-gel mCherry fluorescence imaging in Figure S4B shows that LAP–mCherry runs at the expected molecular weight (27 kD) in negative control samples in which azide 9 or streptavidin are omitted. In lane 1, however, 21% of LAP–mCherry is shifted up to ~80 kD, reflecting binding by streptavidin. We conclude that using the labeling protocol shown in Figure 3A, the two-step labeling yield in cells is approximately 20%.

DISCUSSION

We have developed a methodology for targeting diverse fluorophores to recombinant cellular proteins modified by a 13-amino acid peptide tag (LAP). The targeting is accomplished first by enzyme-mediated alkyl azide ligation and then by strain-promoted cycloaddition with a fluorophore-con-

dx.doi.org/10.1021/ja208090p | J. Am. Chem. Soc. 2012, 134, 3720–3728

jugated cyclooctyne. To develop the method, we systematically optimized the azide ligation reaction through screening of lipoic acid ligase mutants and alkyl azide variants. We then evaluated five different cyclooctyne structures differing in reactivity, selectivity, and extent of nonspecific binding to cells, using a live-cell fluorescein targeting assay. Our final, optimized two-step labeling scheme was used to target a diverse panel of fluorophores ranging from fluorescein to ATTO 647N, to a variety of LAP fusion proteins in multiple mammalian cell lines.

Our comparison of cyclooctynes in cells yielded observations that should prove useful even beyond the context of PRIME, due to the numerous and diverse applications to which cyclooctynes are being applied.[27−32,38,39] One of the earliest cyclooctynes, MOFO (monofluorinated),[20] performed well inside cells, giving signal to background ratios consistently >5:1 in the context of fluorescein targeting to nuclear LAP. This same cyclooctyne was used for cell surface LplA-mediated labeling in our previous study.[19] In next-generation cyclooctynes, fusion to benzene rings increased ring strain and hence the second-order rate constants. Not surprisingly, we found that these cyclooctynes, ADIBO and DIBO, gave ∼4-fold higher absolute signal in cells, compared to MOFO, probably due to increased yield of the cycloaddition product. However, the increase in signal was accompanied by an increase in background, likely due to the greater hydrophobicity and hence nonspecific binding of these probes. Consequently, the signal to background *ratios* were comparable for ADIBO−, DIBO−, and MOFO−fluorescein conjugates.

When we extended the cyclooctyne comparison to other fluorophores, we found that ADIBO and DIBO conjugates to well-behaved hydrophilic fluorophores such as fluorescein and Oregon Green gave satisfactory labeling, but when we tried to target very hydrophobic fluorophores such as ATTO 647N, the combined hydrophobicity of the dye and the cyclooctyne (ADIBO) precluded successful labeling, due to high nonspecific binding. This was alleviated by using the less hydrophobic MOFO instead. Thus MOFO−ATTO 647N but not ADIBO−ATTO 647N was used to label and image actin in living COS-7 cells. Our study illustrates the need for new cyclooctyne probes that combine high reactivity (as displayed by ADIBO) with low hydrophobicity/nonspecific binding (as displayed by MOFO). In this regard, bicyclononynes (BCNs) show promise.[40] Alternatively, fluorogenic cyclooctynes[41] could be extremely helpful, hiding nonspecific binding, and producing fluorescence only upon specific reaction with azide-conjugated LAP.

Several of the fluorophores targeted using LplA and strain-promoted cycloaddition in this study have exemplary properties that make them attractive alternatives to fluorescent proteins. For instance, X-rhodamine is a bright and photostable fluorophore commonly used for speckle imaging of actin.[42] ATTO 647N is one of the best fluorophores of any kind for both STED (stimulated emission depletion)[43,44] and STORM-type[17] super-resolution microscopies. On the cell surface, we targeted Alexa Fluor 647, an excellent fluorophore that has been used for countless ensemble and single-molecule imaging experiments. If methods can be developed to deliver sulfonated fluorophores—which include the cyanine dyes and Alexa Fluors—across cell membranes,[45] then these too should be targetable to specific intracellular proteins using PRIME.

In this work, we focus on the use of strain-promoted cycloaddition to accomplish two-step fluorophore targeting, but the availability of new and improved bio-orthogonal ligation chemistries opens up alternative possibilities. In separate work, we demonstrate two-step fluorophore targeting using LplA in combination with Diels−Alder cycloaddition between a *trans*-cyclooctene and tetrazine.[46] The very fast cycloaddition kinetics ($k \sim 10^4\ M^{-1}\ s^{-1}$) yields substantial improvements in signal to background ratio for intracellular protein labeling. Another interesting advance is in copper-catalyzed click chemistry. Previously discounted for cellular applications due to copper toxicity, new improvements in copper ligand design and reactive oxygen species scavenging have made it possible to perform click chemistry on live cell surfaces and even animals.[24] If the toxicity can be further reduced, while preserving the fast kinetics of ligation (currently 10^4−10^7 fold greater than strain-promoted cycloaddition[25]), then copper-catalyzed click chemistry will be competitive with other methods for bio-orthogonal derivatization on the cell surface.

Considered in the context of other protein labeling methods,[3] the disadvantages of the approach presented here are the requirement for coexpression of the LplA labeling enzyme, the unavoidable background caused by nonspecific binding of cyclooctyne−fluorophore conjugates (albeit low in the case of hydrophilic fluorophores such as fluorescein and Oregon Green), and the signal which is fundamentally limited by the kinetics of strain-promoted cycloaddition chemistry. Given these factors, the methodology will be most useful as a nontoxic (in contrast to FlAsH[6]) labeling method for abundant proteins, whose fusion to large tags (such as fluorescent proteins, HaloTag,[4], or SNAP tag[5]) perturb function, such as actin.

■ ASSOCIATED CONTENT

Supporting Information

Figures S1−S6, experimental procedures for the synthesis of alkyl azides and cyclooctyne−fluorophore conjugates, plasmid construction, immunofluorescence detection of LplA, kinetic analysis of azide 9 ligation by ^{W37I}LplA, measurement of ligation yields, cell surface labeling, and quantitative analysis of cell images. Complete reference 4 with all authors' names listed. This material is available free of charge via the Internet at http://pubs.acs.org.

■ AUTHOR INFORMATION

Corresponding Author

ating@mit.edu

■ ACKNOWLEDGMENTS

Hemanta Baruah and Marta Fernández-Suárez performed preliminary experiments. We thank Daniel Liu, Justin Cohen, and Katie White for plasmids and helpful discussions. DIBO−Oregon Green 488 diacetate was a gift from Kyle Gee (Life Technologies). This work was supported by the National Institutes of Health (R01 GM086214), the Dreyfus Foundation, the American Chemical Society, and MIT.

■ REFERENCES

(1) Fernández-Suárez, M.; Ting, A. Y. *Nat. Rev. Mol. Cell Biol.* **2008**, *9*, 929−943.
(2) Huang, B.; Babcock, H.; Zhuang, X. W. *Cell* **2010**, *143*, 1047−1058.
(3) Wombacher, R.; Cornish, V. W. *J. Biophoton.* **2011**, *4*, 391−402.
(4) Los, G. V.; et al. *ACS Chem. Biol.* **2008**, *3*, 373−382.
(5) Gautier, A.; Juillerat, A.; Heinis, C.; Correa, I. R.; Kindermann, M.; Beaufils, F.; Johnsson, K. *Chem. Biol.* **2008**, *15*, 128−136.

(6) Griffin, B. A.; Adams, S. R.; Tsien, R. Y. *Science* **1998**, *281*, 269−272.
(7) Uttamapinant, C.; White, K. A.; Baruah, H.; Thompson, S.; Fernandez-Suarez, M.; Puthenveetil, S.; Ting, A. Y. *Proc. Natl. Acad. Sci. U.S.A.* **2010**, *107*, 10914−10919.
(8) Stroffekova, K.; Proenza, C.; Beam, K. *Pflugers Arch. Ges. Phys.* **2001**, *442*, 859−866.
(9) Popp, M. W. L.; Ploegh, H. L. *Angew. Chem., Int. Ed.* **2011**, *50*, 5024−5032.
(10) Zhou, Z.; Cironi, P.; Lin, A. J.; Xu, Y.; Hrvatin, S.; Golan, D. E.; Silver, P. A.; Walsh, C. T.; Yin, J. *ACS Chem. Biol.* **2007**, *2*, 337−346.
(11) Wu, P.; Shui, W. Q.; Carlson, B. L.; Hu, N.; Rabuka, D.; Lee, J.; Bertozzi, C. R. *Proc. Natl. Acad. Sci. U.S.A.* **2009**, *106*, 3000−3005.
(12) Cronan, J. E. *Adv. Microb. Physiol.* **2005**, *50*, 103−146.
(13) Puthenveetil, S.; Liu, D. S.; White, K. A.; Thompson, S.; Ting, A. Y. *J. Am. Chem. Soc.* **2009**, *131*, 16430−16438.
(14) Jin, X.; Uttamapinant, C.; Ting, A. Y. *ChemBioChem* **2011**, *12*, 65−70.
(15) Cohen, J. D.; Thompson, S.; Ting, A. Y. *Biochemistry* **2011**, *50*, 8221−8225.
(16) Baruah, H.; Puthenveetil, S.; Choi, Y. A.; Shah, S.; Ting, A. Y. *Angew. Chem., Int. Ed.* **2008**, *47*, 7018−7021.
(17) Dempsey, G. T.; Vaughan, J. C.; Chen, K. H.; Bates, M.; Zhuang, X. *Nat. Methods* **2011**, *8*, 1027−1036.
(18) Fujiwara, K.; Maita, N.; Hosaka, H.; Okamura-Ikeda, K.; Nakagawa, A.; Taniguchi, H. *J. Biol. Chem.* **2010**, *285*, 9971−9980.
(19) Fernández-Suárez, M.; Baruah, H.; Martinez-Hernandez, L.; Xie, K. T.; Baskin, J. M.; Bertozzi, C. R. *Nat. Biotechnol.* **2007**, *25*, 1483−1487.
(20) Agard, N. J.; Baskin, J. M.; Prescher, J. A.; Lo, A.; Bertozzi, C. R. *ACS Chem. Biol.* **2006**, *1*, 644−648.
(21) Debets, M. F.; van Berkel, S. S.; Schoffelen, S.; Rutjes, F. P. J. T.; van Hest, J. C. M.; van Delft, F. L. *Chem. Commun.* **2010**, *46*, 97−99.
(22) Kuzmin, A.; Poloukhtine, A.; Wolfert, M. A.; Popik, V. V. *Bioconjugate Chem.* **2010**, *21*, 2076−2085.
(23) Schilling, C. I.; Jung, N.; Biskup, M.; Schepers, U.; Brase, S. *Chem. Soc. Rev.* **2011**, *40*, 4840−4871.
(24) del Amo, D. S.; Wang, W.; Jiang, H.; Besanceney, C.; Yan, A. C.; Levy, M.; Liu, Y.; Marlow, F. L.; Wu, P. *J. Am. Chem. Soc.* **2010**, *132*, 16893−16899.
(25) Sletten, E. M.; Bertozzi, C. R. *Acc. Chem. Res.* **2011**, *44*, 666−676.
(26) Hong, V.; Steinmetz, N. F.; Manchester, M.; Finn, M. G. *Bioconjugate Chem.* **2010**, *21*, 1912−1916.
(27) Beatty, K. E.; Fisk, J. D.; Smart, B. P.; Lu, Y. Y.; Szychowski, J.; Hangauer, M. J.; Baskin, J. M.; Bertozzi, C. R. *ChemBioChem* **2010**, *11*, 2092−2095.
(28) Beatty, K. E.; Szychowski, J.; Fisk, J. D.; Tirrell, D. A. *ChemBioChem* **2011**, *12*, 2137−2139.
(29) Plass, T.; Milles, S.; Koehler, C.; Schultz, C.; Lemke, E. A. *Angew. Chem., Int. Ed.* **2011**, *50*, 3878−3881.
(30) Baskin, J. M.; Prescher, J. A.; Laughlin, S. T.; Agard, N. J.; Chang, P. V.; Miller, I. A.; Lo, A.; Codelli, J. A.; Bertozzi, C. R. *Proc. Natl. Acad. Sci. U.S.A.* **2007**, *104*, 16793−16797.
(31) Laughlin, S. T.; Baskin, J. M.; Amacher, S. L.; Bertozzi, C. R. *Science* **2008**, *320*, 664−667.
(32) Chang, P. V.; Prescher, J. A.; Sletten, E. M.; Baskin, J. M.; Miller, I. A.; Agard, N. J.; Lo, A.; Bertozzi, C. R. *Proc. Natl. Acad. Sci. U.S.A.* **2010**, *107*, 1821−1826.
(33) Sletten, E. M.; Bertozzi, C. R. *Org. Lett.* **2008**, *10*, 3097−3099.
(34) Sanders, B. C.; Friscourt, F.; Ledin, P. A.; Mbua, N. E.; Arumugam, S.; Guo, J.; Boltje, T. J.; Popik, V. V.; Boons, G. J. *J. Am. Chem. Soc.* **2011**, *133*, 949−957.
(35) Codelli, J. A.; Baskin, J. M.; Agard, N. J.; Bertozzi, C. R. *J. Am. Chem. Soc.* **2008**, *130*, 11486−11493.
(36) Jewett, J. C.; Sletten, E. M.; Bertozzi, C. R. *J. Am. Chem. Soc.* **2010**, *132*, 3688−3690.
(37) Stockmann, H.; Neves, A. A.; Stairs, S.; Ireland-Zecchini, H.; Brindle, K. M.; Leeper, F. J. *Chem. Sci.* **2011**, *2*, 932−936.
(38) Jayaprakash, K. N.; Peng, C. G.; Butler, D.; Varghese, J. P.; Maier, M. A.; Rajeev, K. G.; Manoharan, M. *Org. Lett.* **2010**, *12*, 5410−5413.
(39) Bostic, H. E.; Smith, M. D.; Poloukhtine, A. A.; Popik, V. V.; Best, M. D. *Chem. Commun.* **2012**, *48*, 1431−1433.
(40) Dommerholt, J.; Schmidt, S.; Temming, R.; Hendriks, L. J.; Rutjes, F. P.; van Hest, J. C.; Lefeber, D. J.; Friedl, P.; van Delft, F. L. *Angew. Chem. Int. Ed.* **2010**, *49*, 9422−9425.
(41) Jewett, J. C.; Bertozzi, C. R. *Org. Lett.* **2011**, *13*, 5937−5939.
(42) Lim, J. I.; Sabouri-Ghomi, M.; Machacek, M.; Waterman, C. M.; Danuser, G. *Exp. Cell Res.* **2010**, *316*, 2027−2041.
(43) Mueller, V.; Ringemann, C.; Honigmann, A.; Schwarzmann, G.; Medda, R.; Leutenegger, M.; Polyakova, S.; Belov, V. N.; Hell, S. W.; Eggeling, C. *Biophys. J.* **2011**, *101*, 1651−1660.
(44) Westphal, V.; Rizzoli, S. O.; Lauterbach, M. A.; Kamin, D.; Jahn, R.; Hell, S. W. *Science* **2008**, *320*, 246−249.
(45) Pauff, S. M.; Miller, S. C. *Org. Lett.* **2011**, *13*, 6196−6199.
(46) Liu, D. S.; Tangpeerachaikul, A.; Selvaraj, R.; Taylor, M. T.; Fox, J. M.; Ting, A. Y. *J. Am. Chem. Soc.* **2012**, *134*, 792−795.